



# Computational determination of binding structures and free energies of glucose 6-phosphate dehydrogenase with novel steroid inhibitors

Zhi-Bo Zhao, Yang Liu, Yuan Yao\*

State Key Laboratory of Urban Water Resource and Environment, Academy of Fundamental and Interdisciplinary Science, Harbin Institute of Technology, Harbin 150080, People's Republic of China

## ARTICLE INFO

### Article history:

Accepted 23 May 2014

Available online 2 June 2014

### Keywords:

Glucose 6-phosphate dehydrogenase

Binding mode

Binding free energy

Molecular docking

Molecular dynamics simulation

MM-PBSA

## ABSTRACT

Glucose 6-phosphate dehydrogenase (G6PD), the first and the rate-limiting enzyme in the pentose phosphate pathway (PPP), catalyzes the oxidation of G6P to 6-phosphogluconolactone and the reduction of NADP<sup>+</sup> to NADPH. Its key role in cancer promotes the development of a potent and selective inhibitor that might increase cancer cell death when combined with radiotherapy. In the present study, we investigated the detailed binding modes and binding free energies for G6PD interacting with a promising series of recently developed inhibitors, i.e., the steroid derivatives, by performing molecular docking, molecular dynamics (MD) simulations, and binding free energy calculations. The docking indicates that the inhibitors occupy the binding sites of both G6P and NADP<sup>+</sup>. The calculated binding free energies on the basis of the MD-simulated enzyme–inhibitor complexes are in good agreement with the experimental activity data for all of the examined inhibitors. The valuable insights into the detailed enzyme–inhibitor binding including the important intermolecular interactions, e.g., the hydrogen bond interaction and the hydrophobic interaction, have been provided. The computational results provide new insights into future rational design of more potent inhibitors of G6PD as a treatment for cancer.

© 2014 Elsevier Inc. All rights reserved.

## 1. Introduction

In recent years, the role of metabolism in the development and maintenance of cancer has been widely studied. Many metabolic reactions can both quickly generate adenosine triphosphate (ATP) and feed the requirement for new lipids and nucleotides, leading the unrestricted proliferation of tumors. The pentose phosphate pathway (PPP), conserved in humans, animals, plants and microorganisms, is an important pathway involved in the metabolite production. Through this pathway, the substrate, glucose 6-phosphate (G6P), is converted to ribulose 5-phosphate (Ru5-P), used for the synthesis of nucleotide and the reduced form of nicotinamide adenine dinucleotide phosphate (NADPH) is also generated. NADPH not only is involved in macromolecular biosynthesis as a cofactor for many enzymes, but also plays the important role in maintaining the activity of antioxidants, protecting cells against reactive oxygen species (ROS) generated in rapid proliferation of cells.

Glucose 6-phosphate dehydrogenase (G6PD, EC1.1.1.49) is the first and the rate-limiting enzyme in the PPP and catalyzes the oxidation of G6P to 6-phosphogluconolactone and the reduction of NADP<sup>+</sup> to NADPH. In the past years, the importance of G6PD in cancer has been highlighted. In normal cells, the expression of G6PD enzyme is tightly controlled [1]. However, G6PD is overexpressed in many tumors, resulting in a remarkable increase of the G6PD activity in a variety of swollen tumor tissues, including bladder cancer [2], renal cell carcinoma [3], ovarian cancer [4], fiber meat tumor [5], breast cancer [6], endometrial cancer [7], cervical cancer [8], prostate cancer [9,10], and lung cancer [11]. In contrast, tumor cells with low G6PD activity grow more slowly and exhibit enhanced apoptosis [12,13].

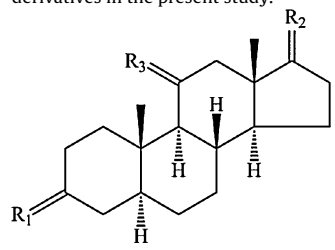
Due to the close relationship between G6PD with cancer, new anticancer drugs which can inhibit the activity of G6PD could be designed by through two different directions, including silencing the gene expression of G6PD to prevent the generation of G6PD [13,14] and discovering the effective compounds against the enzymatic activity of G6PD [15,16]. A competitive G6PD inhibitor, 6-aminonicotinamide (6AN), was used for chemotherapy of various cancers, but had severe side effects, including nerve damage and vitamin B deficiency [15]. Steroids including dehydroepiandrosterone (DHEA) and epiandrosterone (EA) were reported to uncompetitively inhibit G6PD activity in 1960 [17].

\* Corresponding author at: Institute of Theoretical and Simulation Chemistry, Academy of Fundamental and Interdisciplinary Science, Harbin Institute of Technology, 2 Yikuang Street, Harbin 150080, People's Republic of China. Tel.: +86 451 86403305.

E-mail address: [yyuan@hit.edu.cn](mailto:yyuan@hit.edu.cn) (Y. Yao).

**Table 1**

Molecular structures and G6PD inhibitory activities of 6 representative steroid DHEA derivatives in the present study.



| Compound | R <sub>1</sub>          | R <sub>2</sub>                           | R <sub>3</sub> | IC <sub>50</sub> (μM) |
|----------|-------------------------|--|----------------|-----------------------|
| 1        | α-H, β-OH               | α-H, β-COCH <sub>2</sub> OH              | H <sub>2</sub> | 0.9                   |
| 2        | α-H, β-OH               | α-OH, β-COCH <sub>2</sub> OH             | H <sub>2</sub> | 5.2                   |
| 3        | α-H, β-OH               | α-OH, β-COCH <sub>3</sub>                | O              | 47                    |
| 4        | α-H, β-OH               | α-H, β-CH <sub>2</sub> COCH <sub>3</sub> | H <sub>2</sub> | >200                  |
| 5        | α-NH <sub>2</sub> , β-H | O  | H <sub>2</sub> | >200                  |
| 6        | α-OH, β-H               | O  | H <sub>2</sub> | >200                  |

However, clinical trials with DHEA were unsuccessful because of the required high oral doses and the conversion of DHEA into the active androgens [18]. Some attempts have been performed to improve the activity through synthetic modification [19,20] and electrostatic potential map analysis [21], resulting in the discovery of 16α-bromo substituent of DHEA and EA with the remarkably increased inhibition activity. However, none has a remarkable selectivity for inhibiting G6PD among these reported molecules [15,16]. Recently, Hamilton et al. designed novel derivatives of the steroid DHEA with approximately 10-fold improved inhibition activity against G6PD [22].

In order to design more potential inhibitors, it is fundamental and necessary to reveal the detailed binding modes of G6PD with these inhibitors and understand the key interactions in the binding. The detailed analysis on the reported G6PD inhibitors indicated that G6PD inhibitory activity requires a β-alcohol group at R<sub>1</sub> position and a ketone group at R<sub>2</sub> position as shown in Table 1 [22]. In order to reveal the important role of these substituent groups on the binding, six steroid DHEA derivatives which meet this structural requirement were selected in the present study and they have an adequate structural variability and a large inhibitory activity range. First, the selected inhibitors were docked into G6PD in a bound state. Then molecular dynamics (MD) simulations and binding free energy calculations were performed to refine the binding structures and to understand the structure–activity relationship of the G6PD inhibitors. A detailed analysis of the determined binding modes and binding free energies provides valuable insights into the structure–activity relationship and may guide future design of more potent G6PD inhibitors.

## 2. Computational details

### 2.1. Structure preparation

The initial model of G6PD was constructed on the basis of the crystal structure of the complex of human G6PD with G6P (PDB code 2BHL) [23]. All small molecules in the crystal structure were removed except the crystal water molecules. The G6PD inhibitors examined in the present study are steroid DHEA derivatives [22]. Their molecular structures and IC<sub>50</sub> values are listed in Table 1. The partial atomic charges for the atoms in these inhibitors were calculated by using the RESP protocol implemented in the Antechamber module in AMBER9 package [24,25] after electrostatic potential (ESP) calculation at HF/6-31G\* level using Gaussian03 program [26].

### 2.2. Molecular docking

The docking program AUTODOCK4.2 with the genetic algorithm method was used to perform the automated molecular docking to explore the binding mode of G6PD with the molecules. All hydrogen atoms in the enzyme were removed except the polar hydrogen atoms. The grid box dimensions were set as 60 Å × 60 Å × 60 Å around the active site and the grid spacing was 0.375 Å. GA population size and maximum number of energy evaluations were set as 150 and 250,000, respectively. The docked structures were examined, and the best pose for each inhibitor was selected on the basis of the docking score, the scaffold conformation and hydrogen bonds formed between the active site residues and the inhibitor. Finally, the inhibitor conformation with the highest top-score was subjected to energy minimizations and MD simulations.

### 2.3. Molecular dynamics simulation

All missing hydrogen atoms and Na<sup>+</sup> counterions were added by LEaP module in AMBER9 package [24,25]. After that each system was solvated in an orthorhombic box of TIP3P water molecules [27] with a minimal solute–wall distance of 10 Å. The prepared system was fully energy minimized followed by the equilibration through gradual increase of the temperature from 10 to 298.15 K. The production MD simulation was subsequently kept running for ~10 ns. During MD simulation, the time step was 2 fs and the cutoff value for nonbond interactions was 10 Å. The Shake procedure [28,29] was employed to constrain all bonds involving hydrogen atoms. All MD simulations were performed by the Sander module in AMBER9 package [24,25].

### 2.4. Binding free energies calculations

The Molecular Mechanics–Poisson–Boltzmann Surface Area (MM–PBSA) method [30] was used to calculate the binding free energies [31–34]. In MM–PBSA method, the free energy of the enzyme–inhibitor binding, ΔG<sub>bind</sub>, is the difference between the free energies of protein–substrate complex (G<sub>cpx</sub>) and the unbound receptor/protein (G<sub>rec</sub>) and ligand (G<sub>lig</sub>) as following:

$$\Delta G_{\text{bind}} = G_{\text{cpx}} - G_{\text{rec}} - G_{\text{lig}} \quad (1)$$

The binding free energy (ΔG<sub>bind</sub>) is the sum of the changes in the molecular mechanical (MM) gas-phase binding energy (ΔE<sub>MM</sub>), solvation free energy (ΔG<sub>solv</sub>), and entropic contribution (−TΔS):

$$\Delta G_{\text{bind}} = \Delta E_{\text{MM}} + \Delta G_{\text{solv}} - T\Delta S \quad (2)$$

The molecular mechanical energy ΔE<sub>MM</sub> is further divided into the internal energy (ΔE<sub>int</sub>), the Coulomb energy (ΔE<sub>ele</sub>), the van der Waals energy (ΔE<sub>vdW</sub>) in gas phase:

$$\Delta E_{\text{MM}} = \Delta E_{\text{int}} + \Delta E_{\text{ele}} + \Delta E_{\text{vdW}} \quad (3)$$

The solvation free energy is divided into a polar part (ΔG<sub>PB</sub>) and a nonpolar part (ΔG<sub>np</sub>)

$$\Delta G_{\text{solv}} = \Delta G_{\text{PB}} + \Delta G_{\text{np}} \quad (4)$$

Here, the polar contribution (ΔG<sub>PB</sub>) is calculated by solving the Poisson–Boltzmann (PB) equation [35] as implemented in AMBER9 package [24,25]. The value of the interior dielectric constant and exterior dielectric constant were set to 1 and 80, respectively. The nonpolar solvation energy (ΔG<sub>np</sub>) was calculated from the solvent-accessible surface area (SASA) using the hard-sphere atomic model. The probe radius of the solvent was set to 1.4 Å. ΔG<sub>np</sub> is calculated using

$$\Delta G_{\text{np}} = \gamma \cdot \Delta \text{SASA} + \beta \quad (5)$$

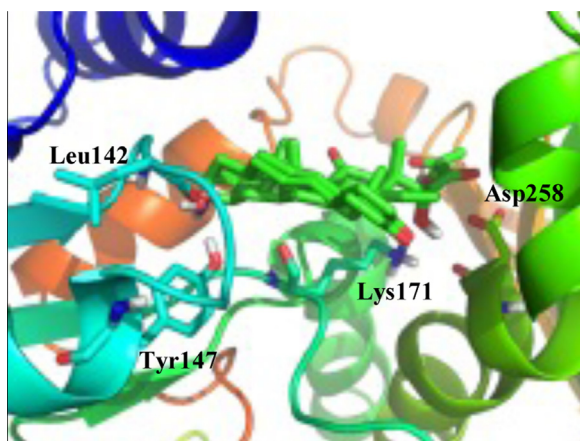


Fig. 1. Superposition of the docked binding structures for 6 inhibitors.

where the surface tension  $\gamma$  and the offset  $\beta$  were set to the standard values of 0.00542 kcal/mol Å<sup>2</sup> and 0.92 kcal/mol, respectively.

The entropic contribution to the binding free energy ( $-T\Delta S$ ) was obtained by performing Normal-Mode Analysis (NMA) in AMBER9 package [24,25].

For each MD-simulated G6PD-inhibitor complex, the  $\Delta G_{\text{bind}}$  values were calculated for the 100 snapshots of the MD trajectory (one snapshot for each 2 ps during the last 200 ps of the stable trajectory) and the final  $\Delta G_{\text{bind}}$  value was the average of the calculated  $\Delta G_{\text{bind}}$  values for these snapshots.

### 3. Results and discussion

#### 3.1. Binding mode and binding free energies

Six representative steroid DHEA derivatives were selected in the present study because they have an adequate structural variability and a large inhibitory activity range. The binding modes of these inhibitors have been explored by performing molecular docking, followed by MD simulations. Superposition of the docked binding conformations for 6 inhibitors is shown in Fig. 1. As shown in Fig. 1, one can see that all the inhibitors with the same scaffold have the similar binding conformation. They occupy the binding sites of both NADP<sup>+</sup> and G6P, forming the stable enzyme-inhibitor complexes through strong hydrogen bond interactions with several binding site residues. The hydroxyl or amino groups substituted at R<sub>1</sub> position in inhibitors 1–6 form two hydrogen bonds with Leu142 and Tyr147 residues which locates at the NADP<sup>+</sup> binding site [22]. The  $\alpha$ -hydroxyl group substituted at R<sub>2</sub> position in inhibitors 2 and 3 forms two hydrogen bonds with Lys171 and Asp258 residues which locate at the G6P binding site [22]. Notably,  $\beta$ -substituent group at R<sub>2</sub> position in inhibitor 1 can also form hydrogen bonds with Lys171 and Asp258 residues as that in inhibitors 2 and 3 although  $\alpha$ -position of R<sub>2</sub> is substituted by a hydrogen atom. By contrast, substituent groups at R<sub>2</sub> position in inhibitors 4–6 cannot form any hydrogen bond with G6PD. Favorably, these hydrogen bonds between G6PD and the inhibitors play key role in orientating the binding position of the inhibitors. In addition, for inhibitor 3, the oxygen atom substituted at R<sub>3</sub> position cannot form any hydrogen bond with G6PD, playing a weak role in the binding. Plots of MD-simulated internuclear distances and RMSD for C $\alpha$  atoms versus simulation time for each of the G6PD-inhibitor complex shown in Figs. 2 and 3 indicate that each of the G6PD-inhibitor complex is very stable.

As mentioned above, each of the G6PD-inhibitor complex is very stable during ~10 ns MD simulation. So the last 200 ps of the trajectory can reasonably represent the whole trajectory and

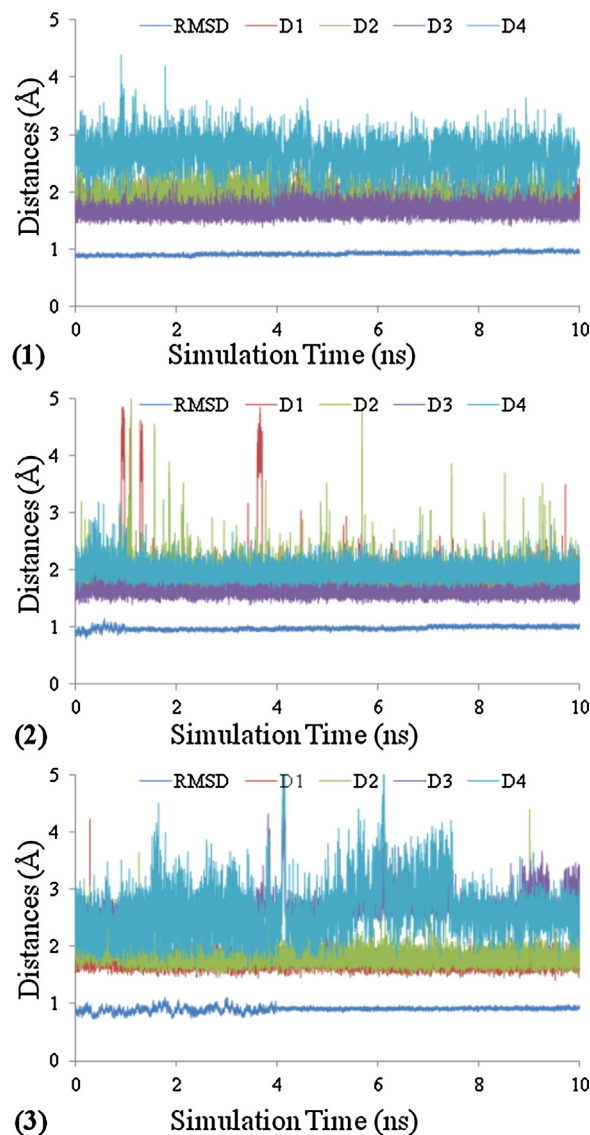


Fig. 2. Plots of MD-simulated internuclear distances and RMSD versus the simulation time for G6PD binding with inhibitors 1–3. Trace D1 represents the internuclear distance between the carbonyl oxygen atom in the Leu142 residue main chain with the hydroxyl or amino group (R<sub>1</sub>). Trace D2 represents the internuclear distance between the hydroxyl hydrogen atom in the Tyr147 residue side chain with the hydroxyl or amino group (R<sub>1</sub>). Trace D3 represents the internuclear distance between the carboxyl oxygen atom in the Asp258 residue side chain with the hydroxyl group (R<sub>2</sub>). Trace D4 represents the internuclear distance between the amino hydrogen atom in the Lys171 side chain with the hydroxyl group (R<sub>2</sub>).

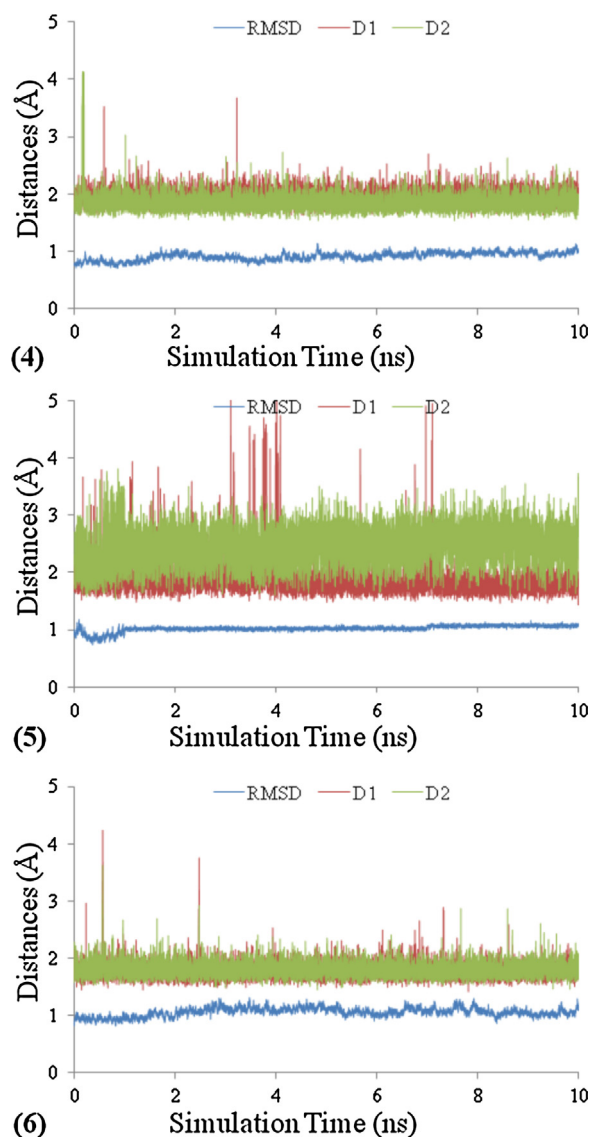
is suitable for the calculation of the binding free energy. The binding free energies of G6PD with the inhibitors calculated by MM-PBSA method based on the MD-simulated binding structures are summarized in Table 2. As listed in Table 2, one can see that

Table 2

The calculated binding free energies (all in kcal/mol).

| Inhibitor | Polar contribution      |                        | Nonpolar contribution   |                        | $-T\Delta S$ | $\Delta G_{\text{bind}}$ |
|-----------|-------------------------|------------------------|-------------------------|------------------------|--------------|--------------------------|
|           | $\Delta E_{\text{ele}}$ | $\Delta G_{\text{PB}}$ | $\Delta E_{\text{vdw}}$ | $\Delta G_{\text{np}}$ |              |                          |
| 1         | −40.44                  | 54.20                  | −34.32                  | −5.18                  | 17.53        | −8.21                    |
| 2         | −44.90                  | 60.77                  | −34.17                  | −5.33                  | 16.45        | −7.18                    |
| 3         | −43.73                  | 58.79                  | −31.51                  | −5.31                  | 15.22        | −6.54                    |
| 4         | −23.85                  | 33.37                  | −26.93                  | −4.32                  | 20.48        | −1.25                    |
| 5         | −4.73                   | 24.02                  | −35.84                  | −4.98                  | 21.24        | −0.29                    |
| 6         | −12.39                  | 25.84                  | −29.43                  | −4.31                  | 18.72        | −1.57                    |





**Fig. 3.** Plots of MD-simulated internuclear distances and RMSD versus the simulation time for G6PD binding with inhibitors 4–6. Trace D1 represents the internuclear distance between the carbonyl oxygen atom in the Leu142 residue main chain with the hydroxyl or amino group ( $R_1$ ). Trace D2 represents the internuclear distance between the hydroxyl hydrogen atom in the Tyr147 residue side chain with the hydroxyl or amino group ( $R_1$ ).

they are all qualitatively consistent with the experimental  $IC_{50}$  values listed in Table 1, demonstrating that our computational results are reasonable and reliable.

### 3.2. Main factors affecting the G6PD-inhibitor binding

It is very important to reveal the main factors affecting the binding and the stability of G6PD-inhibitors complexes. Four residues including Leu142, Tyr147, Lys171 and Asp258 locate the binding sites of G6P and NADP<sup>+</sup> molecules, as mentioned above. Through strong hydrogen bonds formed with these residues, the inhibitors are orientated and stabilized in the binding sites of G6P and NADP<sup>+</sup> molecules, occupying the binding positions of G6P and NADP<sup>+</sup> molecules. This may result in the inhibition of the G6PD activity by the inhibitors. In order to analyze the individual contributions to the binding free energies for 6 inhibitors, the individual polar ( $\Delta E_{ele}$  and  $\Delta G_{pb}$ ) and nonpolar ( $\Delta E_{vdW}$  and  $\Delta G_{np}$ ) contributions are also listed in Table 2. As listed in Table 2, it can

be seen that the major contribution to the binding free energies comes from the nonpolar interaction, particularly the vdW term, for all 6 inhibitors, consistent with the structural feature that the inhibitors are surrounded by several hydrophobic residues (Leu43, Leu142, Pro144, Pro172, Phe250, and Phe253) in G6PD. Compared to the electrostatic term, the solvation free energy from the polar contribution is unfavorable for the binding for inhibitors with G6PD.

### 3.3. Substituent effect

There are three substituent positions in 6 selected inhibitors. For  $R_1$ , both the hydroxyl and the amino groups form strong hydrogen bond with Leu142 and Tyr147 residues in all 6 inhibitors, although they have distinguishable chiral conformations. The heavy atoms (oxygen or nitrogen atoms) in  $R_1$  groups act as a hydrogen bond acceptor to form a strong hydrogen bond with the side chain hydroxyl group in Tyr147 residue, whereas the hydrogen atoms in  $R_1$  groups act as a hydrogen bond donor, forming a strong hydrogen bond with the main chain carbonyl group in Leu142 residue. For  $R_2$ , there are five different substituent groups in 6 inhibitors. The  $\alpha$ -hydroxyl group in inhibitors 2–3 forms two hydrogen bonds with Lys171 and Asp258 residues, playing significant role in the binding. Surprisingly, the  $\beta$ -terminal hydroxyl group of  $R_2$  in inhibitor 1 is flexible and also forms strong hydrogen bonds with Lys171 and Asp258 residues, although  $\alpha$ -hydroxyl group is missing. As we know, the carbonyl group is a good hydrogen bond acceptor. However, this group in inhibitors 5–6 does not form any hydrogen bond with G6PD. The similar situation also happens in the case of inhibitor 4. The missing hydrogen bonds formed with Lys171 and Asp258 residues in inhibitors 4–6 may explain their lower activities.  $R_3$  group cannot form any hydrogen bond, resulting in a low contribution to the binding.

### 3.4. Insights for improving the inhibition activity

The computational results discussed above may provide some new insights for improving the inhibition activity. (1)  $R_1$  and  $R_2$  groups can form strong hydrogen bond interactions with G6PD, playing the significant role in the orientation and the binding of the inhibitors. This interaction needs to be maintained in the future design of the inhibitor. (2) The hydrophobic interaction plays an important role for the binding of the enzyme with the inhibitor. It is consistent with that the nonpolar interaction, particularly the vdW term, contributes more to the binding free energies as shown in Table 2. The introduction of the hydrophobic group in the inhibitor may increase the nonpolar interaction with G6PD. As discussed above, Leu142 residue forms a hydrogen bond with the hydroxyl or amino groups at  $R_1$  position. It may also form hydrophobic interaction with an introduced hydrophobic group at  $R_1$  position, resulting in the increase of the hydrophobic interaction between G6PD with the inhibitors. Notably that one should account for the possible change in the hydrogen bond interaction associated with the change in hydrophobic interactions. In fact, the overall strength of the multiple hydrogen bonds formed with a substituent group might not be stronger than that of a single one [36]. (3) There are several tyrosine and phenylalanine residues locating in the binding site. The introduction of benzol group in the scaffold may form  $\pi$ – $\pi$  stacking interactions between G6PD and the inhibitors, improving the inhibition activity.

## 4. Conclusion

The detailed binding of G6PD with the steroid DHEA derivatives has been studied by performing molecular docking, MD simulations, and binding free energy calculations. The G6PD-inhibitor

binding modes have been determined and the MD-simulated G6PD-inhibitor complexes have revealed important, favorable interactions between the enzyme and the inhibitors, e.g., the hydrogen bond interactions involving R<sub>1</sub> and R<sub>2</sub> substituent groups, and the hydrophobic interactions. The binding free energies have been estimated and they are qualitatively consistent with the experimental activity data for all inhibitors examined in the present study. On the basis of the structural feature and the calculated binding free energies, the substituent effect and main factors affecting the binding have been discussed. The current results provide a solid base for future rational design of more potent inhibitors of G6PD as a treatment for cancer.

## Acknowledgments

This work was supported by the National Natural Science Foundation of China (20973049, 21203041), the Natural Science Foundation of the Heilongjiang province in China (B201301), Open Project of State Key Laboratory of Urban Water Resource and Environment, Harbin Institute of Technology (HC201213, QA201120), the Fundamental Research Funds for the Central Universities (Grant No. HIT. NSRIF. 2013056, and HIT. IBRSEM.201324).

## References

- [1] W. Kuo, J. Lin, T.K. Tang, *Int. J. Cancer* 85 (2000) 857–864.
- [2] F. Ohl, M. Jung, A. Radonić, M. Sachs, S.A. Loening, K.J. Jung, *Urology* 175 (2006) 1915–1920.
- [3] S. Langbein, W.M. Frederiks, A. zur Hausen, J. Popa, J. Lehmann, C. Weiss, P. Alken, J.F. Coy, *Int. J. Cancer* 122 (2008) 2422–2428.
- [4] G.M. Lewandowicz, P. Britt, A.W. Elgie, C.J. Williamson, H.M. Coley, A.G. Hall, J.M. Sargent, *Gynecol. Oncol.* 85 (2002) 298–304.
- [5] W.M. Frederiks, J. van Marle, C. van Oven, B. Comin-Anduix, M.J. Cascante, *Histochem. Cytochem.* 54 (2006) 47–52.
- [6] R. Bokun, J. Bakotin, D. Milasinovic, *Acta Cytol.* 31 (1987) 249–252.
- [7] E.C. Hughes, *Cancer* 38 (1976) 487–502.
- [8] R. Dutu, M. Nedelea, G. Veluda, V. Burculeu, *Acta Cytol.* 24 (1980) 160–166.
- [9] F. Ohl, M. Jung, C. Xu, C. Stephan, A. Rabien, M. Burkhardt, A. Nitsche, G. Kristiansen, S.A. Loening, A. Radonic, K. Jung, *J. Mol. Med. (Berl)* 83 (2005) 1014–1024.
- [10] E.J. Zampella, E.L. Bradley Jr., T.G. Pretlow 2nd, *Cancer* 49 (1982) 384–387.
- [11] S. Dessi, B. Batetta, R. Cherchi, R. Onnis, M. Pisano, P. Pani, *Oncology* 45 (1988) 287–291.
- [12] A. Fico, F. Pagliarunga, L. Cigliano, P. Abrescia, P. Verde, G. Martini, I. Iaccarino, S. Filosa, *Cell Death Differ.* 11 (2004) 823–831.
- [13] D. Li, Y. Zhu, Q. Tang, H. Lu, H. Li, Y. Yang, Z. Li, S. Tong, *Cancer Biother. Radiopharm.* 24 (2009) 81–90.
- [14] P. Jiang, W. Du, X. Wang, A. Mancuso, X. Gao, M. Wu, X. Yang, *Nat. Cell Biol.* 13 (2011) 310–316.
- [15] S.A. Gupta, *Curr. Opin. Investig. Drugs* 9 (2008) 993–1000.
- [16] E.S. Shin, J. Park, J.M. Shin, D. Cho, S.Y. Cho, D.W. Shin, M. Ham, J.B. Kim, T.R. Lee, *Bioorg. Med. Chem.* 16 (2008) 3580–3586.
- [17] P.A. Marks, J. Banks, *Proc. Natl. Acad. Sci. U. S. A.* 46 (1960) 447–452.
- [18] C. Zhang, Z. Zhang, Y. Zhu, S. Qin, *Anti-Cancer Agents Med. Chem.* 14 (2014) 280–289.
- [19] A.T. Cordeiro, O.H. Thiemann, *Bioorg. Med. Chem.* 18 (2010) 4762–4768.
- [20] J.R. Williams, J.C. Boehm, *Steroids* 60 (1995) 699–708.
- [21] M.H. Charlton, C. Thomson, *J. Chem. Soc. Faraday Trans.* 90 (1994) 3533–3537.
- [22] N.M. Hamilton, M. Dawson, E.E. Fairweather, N.S. Hamilton, J.R. Hitchin, D.I. James, S.D. Jones, A.M. Jordan, A.J. Lyons, H.F. Small, G.J. Thomson, I.D. Waddell, D.J. Ogilvie, *J. Med. Chem.* 55 (2012) 4431–4445.
- [23] M. Kotaka, S. Gover, L. Vandeputte-Rutten, S.W.N. Au, V.M.S. Lam, M. Adams, *J. Acta Crystallogr. Sect. D* 61 (2005) 495–504.
- [24] D.A. Case, T.E. Cheatham, T. Darden, H. Gohlke, R. Luo, K.M. Merz, A. Onufriev, C. Simmerling, B. Wang, R.J. Woods, *J. Comput. Chem.* 26 (2005) 1668–1688.
- [25] D.A.D.T.A. Case, T.E. Cheatham, C.L. Simmerling, J. Wang, R.E. Duke, R. Luo, K.M. Merz, D.A. Pearlman, M. Crowley, R.C. Walker, W. Zhang, B. Wang, S. Hayik, A. Roitberg, G. Seabra, K.F. Wong, F. Paesani, X. Wu, S. Brozell, V. Tsui, H. Gohlke, L. Yang, C. Tan, J. Mongan, V. Hornak, G. Cui, P. Beroza, D.H. Mathews, C. Schafmeister, W.S. Ross, P.A. Kollman, *Amber 9*, University of California, San Francisco, 2006.
- [26] M.J. Frisch, G.W. Trucks, H.B. Schlegel, G.E. Scuseria, M.A. Robb, J.R. Cheeseman, J.A. Montgomery Jr., T. Vreven, K.N. Kudin, J.C. Burant, J.M. Millam, S.S. Iyengar, J. Tomasi, V. Barone, B. Mennucci, M. Cossi, G. Scalmani, N. Rega, G.A. Petersson, H. Nakatsuji, M. Hada, M. Ehara, K. Toyota, R. Fukuda, J. Hasegawa, M. Ishida, T. Nakajima, Y. Honda, O. Kitao, H. Nakai, M. Klene, X. Li, J.E. Knox, H.P. Hratchian, J.B. Cross, V. Bakken, C. Adamo, J. Jaramillo, R. Gomperts, R.E. Stratmann, O. Yazyev, A.J. Austin, R. Cammi, C. Pomelli, J.W. Ochterski, P.Y. Ayala, K. Morokuma, G.A. Voth, P. Salvador, J.J. Dannenberg, V.G. Zakrzewski, S. Dapprich, A.D. Daniels, M.C. Strain, O. Farkas, D.K. Malick, A.D. Rabuck, K. Raghavachari, J.B. Foresman, J.V. Ortiz, Q. Cui, A.G. Baboul, S. Clifford, J. Cioslowski, B.B. Stefanov, G. Liu, A. Liashenko, P. Piskorz, I. Komaromi, R.L. Martin, D.J. Fox, T. Keith, M.A. Al-Laham, C.Y. Peng, A. Nanayakkara, M. Challacombe, P.M.W. Gill, B. Johnson, W. Chen, M.W. Wong, C. Gonzalez, J.A. Pople, *Gaussian 03*, Revision E.01, Gaussian, Inc., Wallingford, CT, 2004.
- [27] W.L. Jorgensen, J. Chandrasekhar, J.D. Madura, R.W. Impey, M.L. Klein, *J. Chem. Phys.* 79 (1983) 926–935.
- [28] S. Miyamoto, P.A. Kollman, *J. Comput. Chem.* 13 (1992) 952–962.
- [29] J.P. Ryckaert, G. Ciccotti, H.J.C. Berendsen, *J. Comput. Phys.* 23 (1977) 327–341.
- [30] P.A. Kollman, I. Massova, C. Reyes, B. Kuhn, S. Huo, L. Chong, M. Lee, T. Lee, Y. Duan, W. Wang, O. Donini, P. Cieplak, J. Srinivasan, D.A. Case, T.E. Cheatham, *Acc. Chem. Res.* 33 (2000) 889–897.
- [31] M. Puiatti, J.L. Borioni, M.G. Vallejo, J.L. Cabrera, A.M. Agnese, M.G. Ortega, A.B. Pierini, *J. Mol. Graph. Model.* 44 (2013) 136–144.
- [32] R.N. Shinde, M.E. Sobhia, J. Mol. Graph. Model. 45 (2013) 98–110.
- [33] Y. Zhang, D.B. Pan, Y.L. Shen, N.Z. Jin, H.X. Liu, X.J. Yao, *J. Mol. Model.* 18 (2012) 4517–4527.
- [34] L. Saiz-Urra, M.A. Cabrera, M. Froeyen, *J. Mol. Graph. Model.* 29 (2011) 726–739.
- [35] M.K. Gilson, K.A. Sharp, B.H. Honig, *J. Comput. Chem.* 9 (1988) 327–335.
- [36] B. Yang, A. Hamza, G. Chen, Y. Wang, C.-G. Zhan, *J. Phys. Chem. B* 114 (2010) 16020–16028.